New UWB 1:2 Power Divider with Flat In-Band Splitting and Bandpass Filtering Functions

Thai Hoa Duong · Ihn Seok Kim

Abstract

This paper introduces a new U.S. ultra-wideband(UWB: 3.1～10.6 GHz) 1:2 power divider based on a single section Wilkinson type configuration. The divider provides very flat in-band power splitting, high isolation, low insertion loss, sharp roll-off bandpass filtering, and DC blocking characteristics. The circuit consists of a $\lambda/4$ Y resonator, three capacitively coupled $\lambda/2$ short-circuited lines, and a resistor between the two output ports. The circuit structure was simulated with ADS and HFSS, and realized with low-temperature co-fired ceramic(LTCC) green tape, which has a dielectric constant of 7.8. $|S_{11}|$ better than 10 dB, $|S_{21}|$ and $|S_{31}|$ less than 3.2 dB, with both $|S_{22}|$ and $|S_{32}|$ measured as better than 12 dB for the whole UWB band. Measurement results agree closely with HFSS simulation results. The power divider has a compact size of 4×9×0.6 mm^3.

Key words : Power Divider, Ultra Wideband(UWB), Bandpass Filter(BPF), DC Block, Capacitive Coupling, LTCC.

Ⅰ. Introduction

Many researchers are developing new ultra-wideband (UWB: 3.1～10.6 GHz), high speed, and hand-held wireless communication systems worldwide, as the unlicensed use of UWB has been approved in the United States[1]. Various passive and active components for the spectrum must be available to design a new UWB system. One of the components required for new UWB systems is a power divider. Thus, many research results on UWB power dividers have been published recently[2]~[8]. In order to broaden the bandwidth of a power divider, multi-section and additional resistors are usually adopted. Even in the case of the Wilkinson divider, which is the simplest and the most popular type of power divider, more than three cascading sections and three resistors must be used[2]~[5]. Other structures, such as a T-junction, based on microstrip-slotline transition[6], and broadside-coupled three layers, based on slot coupling[7], had been published. The former introduced a 1:2 divider with a return loss better than 10 dB, isolation greater than 7.5 dB, and average insertion loss of 0.5 dB. The latter presented three-way arbitrary dividers which showed return loss and isolation greater than 17 dB and insertion loss less than 1 dB. All of the aforementioned development results could not provide distinctive bandpass characteristics at the band edges, such as 3.1 and 10.6 GHz. If power dividers with a bandpass filter(BPF) function are used for antenna array, it will be advantageous, because we can mitigate or eliminate BPF function located after/before the dividers. Therefore, [8] tried to introduce a divider with BPF function. However, the divider did not satisfy insertion loss characteristics at the upper end of the UWB band, and a fabrication problem of 0.06 mm gap was involved because of the tight coupling required. For power amplifier applications, a DC blocking function between input and output is usually required, and for hand-held short distance communication applications, compact size and low cost are also necessary properties.

In this paper, a single section 1:2 UWB power divider with DC blocking capability, bandpass filtering function, and a size of 9 mm will be introduced in low-temperature co-fired ceramic(LTCC) technology. In Section Ⅱ,

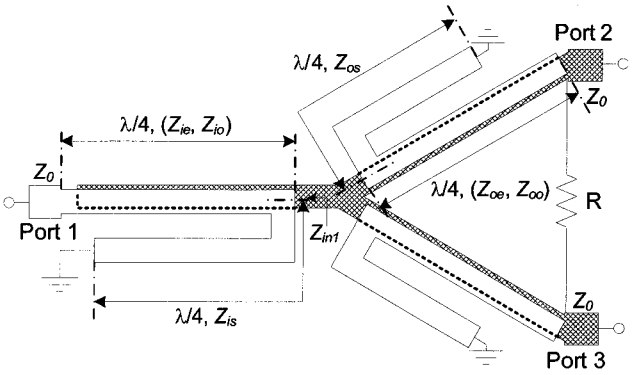

Fig. 1. Proposed UWB power divider with $\lambda/4$ Y resonator(shaded section) and capacitively coupled $\lambda/2$ short-circuited lines(empty sections).

Manuscript received November 27, 2009 ; revised March 3, 2010. (ID No. 20091127-01J)

The Industrial Liaison Research Institute, College of Electronics & Information, Kyunghee University, Yongin, Korea.

$$Z_{in1}=\frac{2Z_0\cos\theta\left[\left(Z_{i+}^2-Z_{i-}^2\right)\cos^2\theta-2Z_{i+}Z_{is}\sin^2\theta\right]+j\sin\theta\left[Z_{i+}\left(Z_{i+}^2-Z_{i-}^2\right)\cos^2\theta+2Z_{is}\left(Z_{i+}^2\cos^2\theta-Z_{i-}^2\right)\right]}{2\sin\theta\left[-Z_{i+}\left(Z_{i+}+2Z_{is}\right)\sin\theta\cos\theta+j2Z_0\left(Z_{i+}\cos^2\theta-2Z_{is}\sin^2\theta\right)\right]} \tag{1}$$

$$Z_{in2}^e=\frac{2Z_0\cos\theta\left[\left(Z_{o+}^2-Z_{o-}^2\right)\cos^2\theta-2Z_{o+}Z_{os}\sin^2\theta\right]+jZ_{o+}\sin\theta\left[\left(Z_{o+}^2-Z_{o-}^2\right)\cos^2\theta-2Z_{os}Z_{o+}\sin^2\theta\right]}{2\left[\cos\theta\left(Z_{o+}^2\cos^2\theta-Z_{o-}^2-2Z_{o+}Z_{os}\sin^2\theta\right)+j2Z_0\sin\theta\left(Z_{o+}\cos^2\theta-2Z_{os}\sin^2\theta\right)\right]} \tag{2}$$

the analysis and design theory for the proposed power divider are presented. For verification, HFSS(High Frequency Structure Simulator) simulation and experimental results for the divider are given and compared in Section Ⅲ.

Ⅱ. Analysis and Design Theory

2-1 Circuit Configuration

The configuration of the 1:2 power divider developed in this paper is shown in Fig. 1. The divider consists of $\lambda/4$ Y resonator with three capacitively coupled $\lambda/2$ short-circuited lines, where λ is the wavelength at the center frequency of 6.85 GHz for the U.S. UWB band. One of three $\lambda/2$ short-circuited lines is used for the input of the divider. One arm of the Y resonator is capacitively coupled with the $\lambda/2$ input short-circuited line and the other two arms of the Y resonator are used as two power splitting lines. The two arms are also capacitively coupled with two $\lambda/2$ short-circuited lines and connected to two 50 Ω output ports, respectively. To obtain good isolation properties between the two output ports, a resistor R is installed. This structure has been designed on a two layer construction in stripline configuration to obtain capacitive coupling as shown in Fig. 1.

2-2 Even and Odd Mode Analyses

The power divider has been designed based on the even and odd mode analysis[9]. The input impedance (Z_{in1}) looking backward to the input at the Y junction when the input port is terminated by Z_0=50 Ω, and is calculated by (1) as shown in Appendix 1, where Z_{i+}= $Z_{ie}+Z_{io}$, $Z_{i-}=Z_{ie}-Z_{io}$, and Z_{ie} and Z_{io} are the even and odd mode characteristic impedances of the input coupled line, respectively. In addition, Z_{is} and Z_{os} are the characteristic impedances of the $\lambda/4$ part not coupled with the arms of the Y resonator at the input port and output port, respectively. Thus, the input section which has the $\lambda/2$ line coupled with the arm can be represented by the impedance Z_{in1} before analyzing the circuit structure with the even and odd mode method.

Fig. 2 shows the one-port circuit model for the proposed power divider when the input port is terminated by Z_0=50 Ω under the even mode excitation. In this case, the symmetrical plane becomes a perfect magnetic wall and the input impedance(Z_{in1}) from (1) doubles ($2Z_{in1}$). Therefore, the even mode input impedance(Z_{in2}^e) looking into the output port at the Y junction can be derived by (2) as shown in Appendix 2, where $Z_{o+}=Z_{oe}+Z_{oo}$, $Z_{o-}=Z_{oe}-Z_{oo}$, and Z_{oe} and Z_{oo} are the even and odd mode characteristic impedances of the input coupled line, respectively.

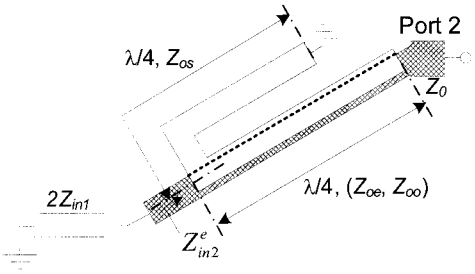

Fig. 2. Even mode circuit model for the proposed power divider.

At the center frequency of 6.85 GHz($\theta=\pi/2$), Z_{in1} and Z_{in2}^e can be simplified as (3) and (4), respectively. To maintain the impedance matching condition, $Z_{in2}^e=2Z_{in1}$, (5) is required.

$$Z_{in1}=\frac{Z_{i-}^2}{4Z_0} \tag{3}$$

$$Z_{in2}^e=\frac{Z_{o+}^2}{4Z_0} \tag{4}$$

$$Z_{oe}+Z_{oo}=\sqrt{2}\left(Z_{ie}-Z_{io}\right) \tag{5}$$

Under the odd-mode excitation, the circuit at the symmetrical plane can be considered as short-circuited, since the strip conductors at the center are a grounded via (virtual electrical wall) as shown in Fig. 3. Therefore, we can obtain the odd mode output impedance(Z_{in2}^o) as (6) and, at the frequency of $\theta=\pi/2$, Z_{in2}^o becomes infinity. Consequently, the impedance matching condition, $1/Z_{in2}^o+2/R=1/Z_0$, provides (7).

$$Z_{in2}^o=j\frac{1}{2}\tan\theta Z_{o+} \tag{6}$$

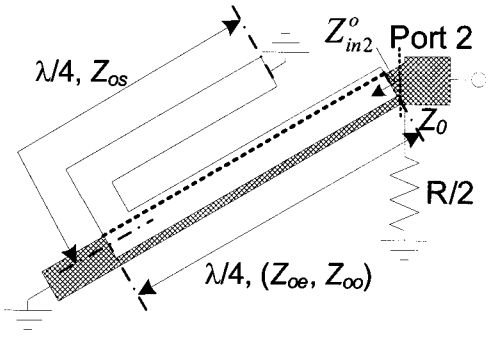

Fig. 3. Odd mode circuit model for the proposed power divider.

$$R=2Z_0 \tag{7}$$

2-3 Design Theory

We need to know that the conditions in (5) and (7) are only accurate at $\theta=\pi/2$ and they are gradually degraded as θ deviates away from $\pi/2$. However, as the coupled $\lambda/2$ short-circuited lines[10] are installed at the input and outputs provide two transmission poles, and the parallel combining effect of the two output coupled line structures adds an additional two poles. As a result, four transmission poles are generated in the passband, two on each side of $\theta=\pi/2$. Thus, a good impedance matching condition can be achieved over the UWB frequency range if these poles are properly allocated. In addition, the two capacitively coupled $\lambda/2$ short-circuited lines installed at the output ports introduced two transmission zeros at the lower and upper transition bands. Positions of transmission zeros can be determined by (8) as shown in Appendix 3.

$$\tan\theta=\sqrt{\frac{2Z_{oe}Z_{oo}}{Z_{os}\left(Z_{oe}+Z_{oe}\right)}} \tag{8}$$

In order to obtain the bandpass property from the divider, the lower/upper cutoff frequencies of the passband can be derived under the definitions of 10-dB magnitudes. Figs. 4(a) and (b) show the two cutoff frequencies of the power divider versus the characteristic impedance Z_{os} of the $\lambda/4$ part of the $\lambda/2$ short-circuited coupled lines, where the $\lambda/4$ part is the section not coupled with the Y resonator, and the coupling coefficient of the coupled lines(C_{out}) at the output ports, respectively. The lower cutoff frequencies are decreased and the higher cutoff frequencies increased as Z_{os} and C_{out} are increased from 22.5 to 55 Ω and from −4.38 to −2.2 dB, respectively. Fig. 4 shows the operational bandwidth for a BPF function. The vertical planes (a-a') and (b-b') with Z_{os}=34.5 Ω and C_{out}=−2.55 dB show the 110 % fractional bandwidth that corresponds to the 3.1-10.6 GHz UWB. If two transmission zeros are placed at 2.9 and 10.8 GHz, respectively, Z_{oe}=83.38 Ω, Z_{oo}=12.16 Ω have been chosen. To obtain good matching conditions, Z_{ie} =83.38 Ω, Z_{io}=13.31 Ω, Z_{is}=45 Ω, and R=100 Ω from (5) and (7) have been used for this study.

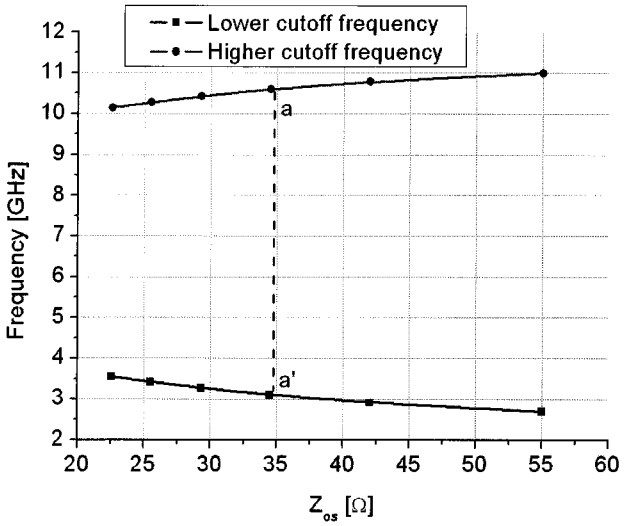

(a)

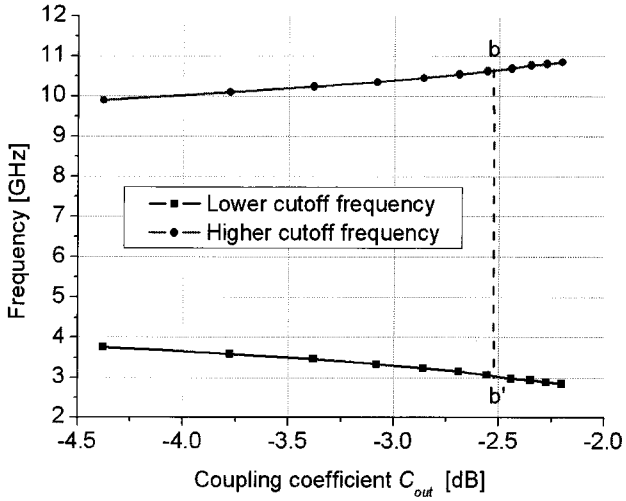

(b)

Fig. 4. Bandwidth property of the proposed power divider depending on (a) The characteristic impedance Z_{os} of the $\lambda/4$ section of the $\lambda/2$ short-circuited line and (b) The coupling coefficient C_{out} of the coupled lines at the output ports.

Fig. 5 shows the ADS simulation results for the proposed power divider. The input return loss($|S_{11}|$) is better than 23 dB and 3 dB power splitting from the input to output ports ($|S_{21}|$, $|S_{31}|$) obtained for the overall UWB band. A greater than 13 dB return loss at output ports ($|S_{22}|$, $|S_{33}|$) and larger than 12 dB isolation between the two output ports ($|S_{32}|$) are achieved for the whole band.

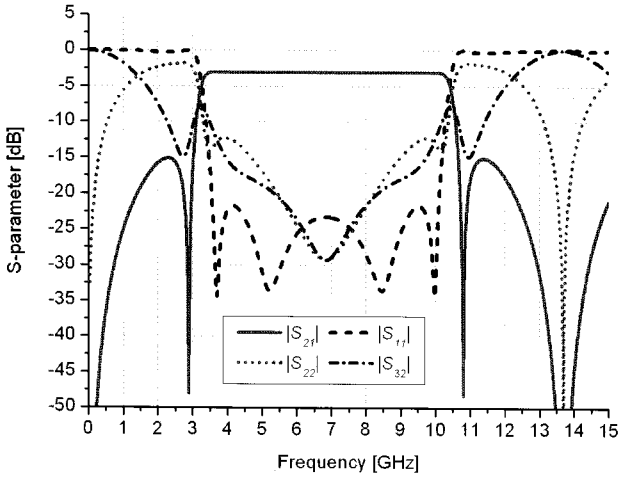

Fig. 5. ADS simulation results for the proposed UWB power divider.

Both attenuation slopes in the lower and upper transition bands are 94 dB/GHz.

III. Field Simulation and Measurement Results

The proposed structure as shown in Fig. 6 was simulated and tuned with the HFSS program(Ansoft v.11). The structure consisted of 14 layers and each layer had a thickness of 43 μm and dielectric constant of 7.8. The circuit patterns were located on the seventh and eighth layers and via walls were added to the structure in place of solid walls in order to reduce the effects of interference. Due to the limitations of our LTCC manufacturing process, the distance between the two adjacent vias needed to be larger than 0.35 mm. This led to a slight deterioration of the performance of the power divider at high frequencies. We measured the divider characteristics with the Anritsu ME7808A network analyzer and the Cascade Microtech Summit 12971B probe station. The measurement results were compared with the simulation results. Input/output striplines were connected to input/output circular ports which have inner and outer diameters of 200 μm and 750 μm, respectively, by solid vias (via's diameter of 120 μm). External chip resistor R=100 Ω were connected into two rectangular pads on the bottom layer of the power divider. Measurement probes with a 400 μm pitch size were used.

Fig. 7 shows the comparisons between the simulation and measurement results of the power divider in term of S-parameters and group delay. The dotted lines indicate the simulation results, and these results show a bandwidth of 7.5 GHz(3.1 ~ 10.6 GHz). The return loss at the input port($|S_{11}|$) is better than 17 dB and an insertion loss($|S_{21}|$, $|S_{31}|$) of less than 3.1 dB over the UWB band as shown in Fig. 7(a). The group delay of the divider is approximately 0.15±0.1 ns for the frequency range

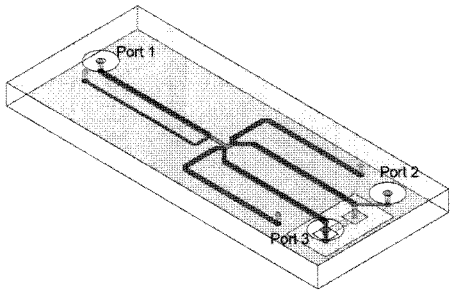

(a) 3-D view

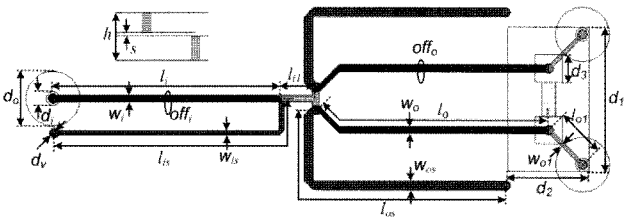

(b) Top view

Fig. 6. The structure of the proposed power divider(w_i= 0.08 mm, l_i=3.37 mm, w_{is}=0.06 mm, l_{is}=3.85 mm, off_i=0 mm, l_{i1}=0.4 mm, w_o=0.1 mm, l_o=3.65 mm, w_{os}=0.13 mm, l_{os}=3.8 mm, off_o=0 mm, w_{o1}=0.08 mm, l_{o1}=0.6 mm, d_1=2.1 mm, d_2=1.2 mm, d_3=0.4 mm, d_i=0.2 mm, d_o=0.7 mm, d_v=0.12 mm, h= 0.6 mm, s=0.043 mm).

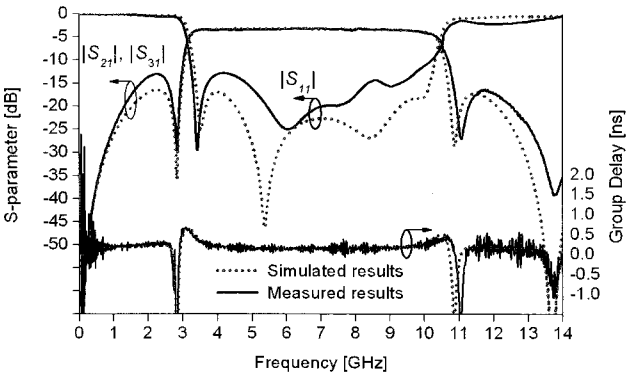

(a) $|S_{11}|$, $|S_{21}|$, and $|S_{31}|$

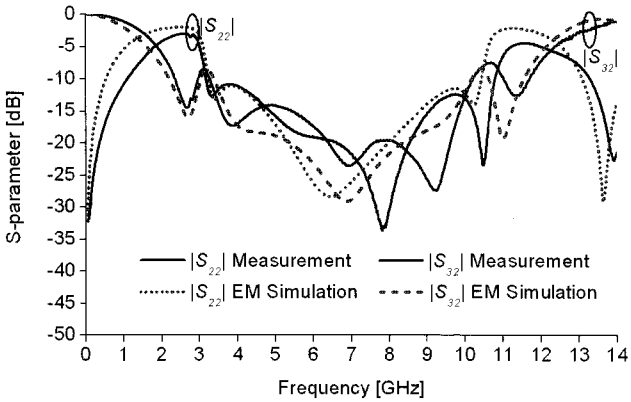

(b) $|S_{22}|$ and $|S_{32}|$

Fig. 7. Comparison of measured and simulated results for the proposed power divider.

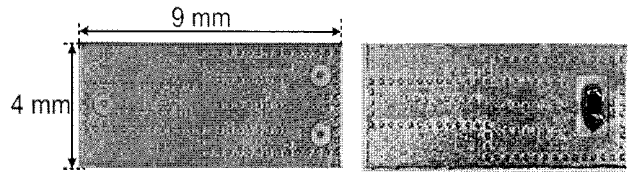

(a) Top view (b) Bottom view

Fig. 8. The fabricated power divider.

from 3.2 GHz to 10.5 GHz. Attenuation slopes in the lower and upper transition bands are 72.5 dB/GHz and 60 dB/GHz, respectively. The power divider has two transmission zeros at 2.83 and 10.9 GHz, respectively, and the return loss at the output ports ($|S_{22}|$, $|S_{33}|$) and isolation between two output ports ($|S_{32}|$) are all better than 12 dB over the UWB band as shown in Fig. 7(b). The solid line shows the measurement results. $|S_{11}|$ better than 10 dB and $|S_{21}|$ and $|S_{31}|$ less than 3.2 dB were measured. The measured group delay varies between 0.1 ns and 0.3 ns for the frequency range from 3.2 GHz to 10.5 GHz. The measured $|S_{22}|$ as well as $|S_{32}|$ were better than 12 dB for the UWB band. The attenuation slopes in the lower and upper transition bands are 60 dB/GHz and 45 dB/GHz, respectively, and the proposed power divider has a compact size ($4\times9\times0.6$ mm^3). Fig. 8 shows the top and bottom views of the fabricated power divider.

Ⅳ. Conclusion

In this paper, we introduced a novel 1:2 UWB power divider with flat in-band power splitting, high isolation, DC blocking capability, and compact size in LTCC technology. By adopting the $\lambda/4$ Y resonator with capacitively coupled $\lambda/2$ short-circuited lines, the power divider can operate over the U.S. UWB frequency range with a sharp roll-off BPF function at the lower and upper transition bands. The analysis and design theory for the proposed divider have been given, and measurement results agree well with simulation results. We expect that the sharp roll-off characteristics and compact structure of the divider will make it very suitable for UWB array antenna and power amplifier systems, particularly in short distance communication applications. We can also expand this technique into a 1:n power divider[11]~[12].

Appendix

1. Impedance of the Input Structure Z_{in1}

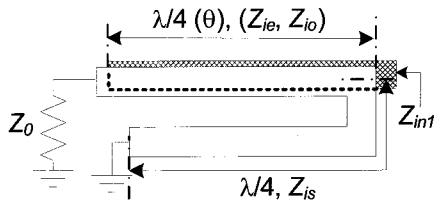

(a)

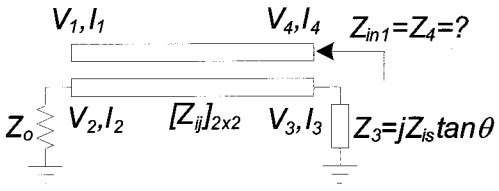

(b)

Fig. A-1. (a) Input structure for the proposed power divider terminated by Z_0=50 Ω and (b) its equivalent 4-port network.

Figs. A-1(a) and (b) show the input structure for the proposed power divider terminated by Z_0=50 Ω and its equivalent 4-port network, respectively, where Z_{ie} and Z_{io} are the even and odd mode characteristic impedances of the coupled line, Z_{is} is the characteristic impedance of the short-circuited stub, Z_3 is the input impedance of the stub, V_i and I_i(i=1.4) are the voltages and currents at port i, respectively, and $[Z_{ij}]_{2\times2}$ is the Z-parameters of the input coupled line which is calculated by (A1), where $Z_{i+}=Z_{ie}+Z_{io}$ and $Z_{i-}=Z_{ie}-Z_{io}$ as [13].

$$\begin{aligned} Z_{11} &= Z_{22} = Z_{33} = Z_{44} = -j\frac{Z_{i+}}{2}\cot\theta \\ Z_{12} &= Z_{21} = Z_{34} = Z_{43} = -j\frac{Z_{i-}}{2}\cot\theta \\ Z_{13} &= Z_{31} = Z_{24} = Z_{42} = -j\frac{Z_{i-}}{2}\csc\theta \\ Z_{14} &= Z_{41} = Z_{23} = Z_{32} = -j\frac{Z_{i+}}{2}\csc\theta \end{aligned} \tag{A1}$$

$$\begin{bmatrix} V_1 \\ -Z_0 I_2 \\ -Z_3 I_3 \\ V_4 \end{bmatrix} = \begin{bmatrix} Z_{11} & Z_{12} & Z_{13} & Z_{14} \\ Z_{21} & Z_{22} & Z_{23} & Z_{24} \\ Z_{31} & Z_{32} & Z_{33} & Z_{34} \\ Z_{41} & Z_{42} & Z_{43} & Z_{44} \end{bmatrix} \begin{bmatrix} 0 \\ I_2 \\ I_3 \\ I_4 \end{bmatrix} \tag{A2}$$

The relationship between the voltages and currents at the 4-port network in Fig. A1(b) can be written by (A2). Therefore, the input impedance $Z_{in1}=V_4/I_4$ can be extracted as (A3), and, by substituting (A1) into (A3), the input impedance Z_{in1} can be obtained as (A4).

$$Z_{in1} = V_4 / I_4 = Z_{42}\frac{Z_{34}Z_{23} - Z_{24}(Z_3 + Z_{33})}{(Z_0 + Z_{22})(Z_3 + Z_{33}) - Z_{32}Z_{23}} + Z_{43}\frac{Z_{34}(Z_0 + Z_{22}) - Z_{24}Z_{32}}{Z_{23}Z_{32} - (Z_3 + Z_{33})(Z_0 + Z_{22})} + Z_{44} \tag{A3}$$

$$Z_{in1}=\frac{2Z_0\cos\theta\left[\left(Z_{i+}^2-Z_{i-}^2\right)\cos^2\theta-2Z_{i+}Z_{is}\sin^2\theta\right]+j\sin\theta\left[Z_{i+}\left(Z_{i+}^2-Z_{i-}^2\right)\cos^2\theta+2Z_{is}\left(Z_{i+}^2\cos^2\theta-Z_{i-}^2\right)\right]}{2\sin\theta\left[-Z_{i+}\left(Z_{i+}+2Z_{is}\right)\sin\theta\cos\theta+j2Z_0\left(Z_{i+}\cos^2\theta-2Z_{is}\sin^2\theta\right)\right]} \tag{A4}$$

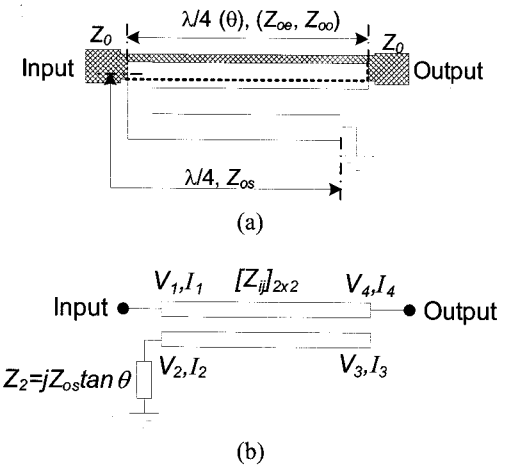

Fig. A-2. (a) Output structure for the proposed power divider and (b) its equivalent 4-port network.

2. Impedance of the Output Structure Z_{in2}^e

Figs. A2(a) and (b) show the output structure for the proposed power divider and its equivalent 4-port network, respectively, where Z_{oe} and Z_{oo} are the even and odd mode characteristic impedances of the coupled line; Z_{os} is the characteristic impedance of the short-circuited stub; Z_2 is the input impedance of the stub; V_i and $I_i(i=1.4)$ are the voltages and currents at port i, respectively; and $[Z_{ij}]_{2\times2}$ is the Z-parameters of the output coupled line(A1), where Z_{o+} and Z_{o+} are replaced by $Z_{i+}=Z_{ie}+Z_{io}$ and $Z_{i-}=Z_{ie}-Z_{io}$.

The relationship between the voltages and currents at the 4-port network in Fig. A2(b) can be written by:

$$\begin{bmatrix}V_1\\-Z_2I_2\\V_3\\V_4\end{bmatrix}=\begin{bmatrix}Z_{11}&Z_{12}&Z_{13}&Z_{14}\\Z_{21}&Z_{22}&Z_{23}&Z_{24}\\Z_{31}&Z_{32}&Z_{33}&Z_{34}\\Z_{41}&Z_{42}&Z_{43}&Z_{44}\end{bmatrix}\begin{bmatrix}I_1\\I_2\\0\\I_4\end{bmatrix} \tag{A5}$$

$$[Z_{2\times2}]^e=\begin{bmatrix}Z_{11}-Z_{12}\dfrac{Z_{21}}{Z_2+Z_{22}}&Z_{14}-Z_{12}\dfrac{Z_{24}}{Z_2+Z_{22}}\\Z_{41}-Z_{42}\dfrac{Z_{21}}{Z_2+Z_{22}}&Z_{44}-Z_{42}\dfrac{Z_{24}}{Z_2+Z_{22}}\end{bmatrix} \tag{A6}$$

$$Z_{in2}^e=Z_{11}^e-\frac{Z_{12}^eZ_{21}^e}{Z_0+Z_{22}^e} \tag{A7}$$

In addition, the Z-parameters $[Z_{2\times2}]^e$ of the output structure in Fig. A2(a) can be derived as (A6). If the output port of the structure is terminated by Z_0=50 Ω, the even mode input impedance Z_{in2}^e can be calculated as (A7) and (A8).

3. Positions of Transmission Zeros

The two capacitively coupled $\lambda/2$ short-circuited lines installed at the output ports at shown in Fig. A2(a) introduce two transmission zeros at the locations of transmission zeros, where $|S_{21}^e|=0$ or $Z_{21}^e=0$. Therefore, we have the relation (A9), and by substituting (A1) into (A9), the positions of transmission zeros can be determined by (A10).

$$Z_{41}-Z_{42}\frac{Z_{21}}{Z_2+Z_{22}}=0 \tag{A9}$$

$$\tan\theta=\sqrt{\frac{2Z_{oe}Z_{oo}}{Z_{os}(Z_{oe}+Z_{oo})}} \tag{A10}$$

The authors wish to acknowledge the financial supprt of LG Innotek and the measurement assistance of the KETI (Korea Electronics Technology Institute).

This work was supported by the 2008 Kyung Hee University sabatical year program.

References

[1] "Revision of part 15 of the commission's rules regarding ultra wideband transmission system", Federal Communications Commission, 2006 [Online]. Available: http://ftp.fcc.gov/oet/info/rules/part15.

[2] S. W. Lee, C. S. Kim, K. S. Choi, J. S. Park, and D. Ahn, "A general design formula of multi-section power divider based on singly terminated filter design theory", *IEEE MTT-S Int. Microwave Symp. Dig.*, vol. 2, pp. 1297-1300, May 2001.

[3] Y. Sun, A. P. Freundorfer, "Broadband folded Wilkin-

$$Z_{in2}^e=\frac{2Z_0\cos\theta\left[\left(Z_{o+}^2-Z_{o-}^2\right)\cos^2\theta-2Z_{o+}Z_{os}\sin^2\theta\right]+jZ_{o+}\sin\theta\left[\left(Z_{o+}^2-Z_{o-}^2\right)\cos^2\theta-2Z_{os}Z_{o+}\sin^2\theta\right]}{2\left[\cos\theta\left(Z_{o+}^2\cos^2\theta-Z_{o-}^2-2Z_{o+}Z_{os}\sin^2\theta\right)+j2Z_0\sin\theta\left(Z_{o+}\cos^2\theta-2Z_{os}\sin^2\theta\right)\right]} \tag{A8}$$

son power combiner/splitter", *IEEE Microwave Wireless Compon. Lett.*, vol. 14, no. 6, pp. 295-297, Jun. 2004.

[4] L. Chiu, T. Y. Yum, Q. Xue, and C. H. Chan, "A wideband compact parallel-strip 180° Wilkinson power divider for push-pull circuitries", *IEEE Microwave Wireless Compon. Lett.*, vol. 16, no. 1, pp. 49-51, Jan. 2006.

[5] H. Oraizi, A.-R. Sharifi, "Design and optimization of broadband asymmetrical multisection Wilkinson", *IEEE Trans. Microwave Theory Tech.*, vol. 54, no. 5, pp. 2220-2231, May 2006.

[6] M. E. Bialkowski, A. M. Abbosh, "Design of a compact UWB out-of-phase power divider", *IEEE Microwave Wireless Compon. Lett.*, vol. 17, no. 4, pp. 289-291, Apr. 2007.

[7] A. M. Abbosh, "Design of ultra-wideband three-way arbitrary power dividers", *IEEE Trans. Microwave Theory Tech.*, vol. 56, no. 1, pp. 194-201, Jan. 2008.

[8] S. W. Wong, L. Zhu, "Ultra-wideband power divider with good in-band splitting and isolation performances", *IEEE Microwave Wireless Compon. Lett.*, vol. 18, no. 8, pp. 518-520, Aug. 2008.

[9] G. L. Zysman, A. K. Johnson, "Coupled transmission line networks in an inhomogeneous dielectric medium", *IEEE Trans. Microwave Theory Tech.*, vol. 17, no. 10, pp. 753-759, Oct. 1969.

[10] T. H. Duong, I. S. Kim, "New elliptic function type UWB BPF based on capacitively coupled lambda/4 open T resonator", *IEEE Trans. Microwave Theory Tech.*, vol. 57, no. 12, Dec. 2009.

[11] I. S. Kim, T. H. Duong, "1:n ultra wideband power divider/combiner based on capacitively coupled n transmission lines with n shorted lines", *Korean Patent, Application No. 10-2009-0046338*, May 2009.

[12] I. S. Kim, T. H. Duong, "1:3 ultra wideband power divider/combiner", *Korean Patent, Application No. 10-2009-0086113*, Sep. 2009.

[13] D. M. Pozar, *Microwave Engineering*, 2nd Ed. New York, Wiley, p. 418, section 8.7, 1998.

Thai Hoa Duong

was born in HCM City, Vietnam in 1981. He received the B.S. degree in Electrical Engineering from Ho Chi Minh City University of Technology, Vietnam in 2004 and his Ph.D. degree in Radio Engineering from the Kyung Hee University, South Korea, in 2010. His research interests include the design, analysis, synthesis and miniaturization of microwave planar ultra wideband passive devices, such as bandpass filters, power divider/combiners, and directional couplers for wireless communication systems.

Ihn Seok Kim(M'82)

was born in Seoul, Korea, on August 4, 1947. He received his B.E. degree in Electrical Engineering from Kyung Hee University in 1974 and his M.Sc. and Ph.D. degrees in Electrical Engineering from the University of Ottawa, Canada, in 1983 and 1991, respectively. From 1973 to 1992, he had worked for Korean Broadcasting Systems as an RF engineer, at Com Dev as technical staff, General Instrument of Canada as a senior engineer, the Canadian Space Agency as a research scientist, and the Korean Mobile Telecommunications Corporation as a senior researcher. In 1992, he joined Kyung Hee University, where he has been working on the modeling of various microwave structures, their applications to filters, power divider/combiners, and microwave oscillators. He also works in the EMI/C field as a member of the Korean delegation for the CISPR B/F and TC 77C committees. From February 1999 to February 2000, he was on sabbatical at ETH (Zurich) and the Motorola EM Lab (Ft. Lauderdale). He served as a reviewer for IEEE MTT from 1998 to the present.